

# Fuzzy Position-Velocity control of Underactuated Finger of FTN Robot Hand

Mirko Raković<sup>a,b,\*</sup>, Govind Anil<sup>c</sup>, Živorad Mihajlović<sup>a</sup>, Srđan Savić<sup>a</sup>, Siddhata Naik<sup>c</sup>, Branislav Borovac<sup>a</sup> and Achim Gottscheber<sup>c</sup>

<sup>a</sup> Faculty of Technical Sciences, University of Novi Sad, Trg Dositeja Obradovića 6, 21000, Novi Sad, Serbia

<sup>b</sup> Institute for Systems and Robotics, Instituto Superior Tecnico, Av. Rovisco Pais 1 6, 1049-001, Lisbon, Portugal

<sup>c</sup> SRH University of Applied Sciences, Ludwig-Guttman-Straße 6, 69123, Heidelberg, Germany

**Abstract.** The significant progress in robotics worldwide, brings further advancements in the design of the mechanical components, miniaturization of sensors and control hardware and more sophisticated control algorithms that come together with more available processing power. The state of the art humanoid robots are usually equipped with dexterous hands. This paper presents the design of the FTN robot hand for humanoid robot MARKO, with the emphasis on the fuzzy logic controller to control the Brushed DC motors used to actuate the underactuated fingers of the hand. The design of the robotic hand is highly anthropomorphic and biologically inspired by the human hands. The hand is passively adaptive to the shape of an object, due to a tendon-driven mechanism and torsional spring in each finger joint. Each of the five fingers has three DOFs (Degrees Of Freedom), except the thumb which has an additional DOF, for the rotation in its base. The fingers are tendon-driven, actuated with five DC motors, embedded in the palm. The proposed fuzzy controller is used to control the position of each finger. The results of the controller are compared with traditional PID control algorithms tuned with Ziegler – Nichols tuning method. The algorithms are first developed in a simulation environment and later are implemented on a real-time ARM Cortex M4 controller.

Keywords: Fuzzy control, BDC motor control, Robotic Hand,

## 1. Introduction

Considering the current trend and goal in robotics research community to provide working and living co-existence of robots and humans, it is necessary to provide the robots with a capability to interact with their environment. The hand plays the most important role in manipulation, which is, together with the ability to move in its environment, the fundamental task of humanoid robots [1-3].

The design of an anthropomorphic robotic hand is a highly challenging task. The robotic hand is a complex mechatronic device whose design has to provide sufficient dexterity, speed and mass/payload ratio in presence of multiple constraints imposed on its weight, size, and packaging. Since our environment and most of the tools and objects are ergonomically designed to fit the shape of human hands it is reasonable to consider a bioinspired

anthropomorphic structure for the design of a robotic hand which would be capable of manipulating objects of different shapes and sizes. In order to use robotic hands in an unstructured environment, they have to possess a certain degree of compliance, to deal with possible impacts and collisions, and passive or active adaptability to different object shapes. Also, the hand should be equipped with force-sensing to manipulate objects of different mechanical characteristics, including fragile objects.

Part of the challenge is the design and implementation of control for robotic hand motion capable of performing robust grasping of common objects in a reliable and repeatable manner, in presence of noise and sensing errors. Despite many research papers and significant progress, this is still considered an open problem. The human hand has around 27 DOFs and it is characterized by great mobility and dexterity. It is very hard to provide a

---

\*Corresponding author. e-mail: rakovicm@uns.ac.rs; rakovicm@isr.tecnico.ulisboa.pt,

compact and functional design for an artificial anthropomorphic hand with so many DOFs since it would demand great volume for actuators. Therefore, many solutions have been proposed for underactuated robotic hands, where several joints are coupled and actuated with a single actuator.

A motor control system can be considered to be good if it can respond to a command instantly without delay and with a high level of accuracy and stability. It should also be able to perform consistently with changes in the operation environment and other parameters. One of the most common classical approaches to control a DC motor is the Proportional – Integral – Derivative controller (PID) controller which uses a feedback loop in order to control the system. PID controllers are used widely in a lot of applications. It is commonly used industrial applications which involve regulation of speed, pressure, temperature etc.

A more intelligent way of controlling a DC motor is to use a Fuzzy logic controller. An advantage of Fuzzy logic control is the fact that it is not required to have (or to identify) the exact mathematical model of the system, i.e. it is a more heuristic approach. Fuzzy logic control algorithm is not composed of mathematical equations, but of a rule base specified by the person designing the controller. It is designed in a way inherently comprehensible to humans. The inputs and outputs are not given as clearly defined values, but instead, membership functions are developed for each input and output in order to specify their degree of membership, and the rule base is used as a lookup in order to generate the output for each condition that arises from the combination of inputs.

### *1.1. State of the art*

After few decades of significant progress in the field of artificial hand design, it is still an open problem with ongoing research. Development of new materials and new types of actuators is also promising for the next generation of robotic hands. Some state of the art solutions for the robotic hand design, characterized by great functionality and dexterity are the Robonaut hand, designed by NASA [4, 5], the series of DLR hands of different generations [6, 7], the GIFU hand III [8], the UB Hand III [9], Shadow Hand [10] and Elumotion Hand 2 [11]. A common drawback of these robotic hands is their complex design and extremely high price. Mostly they are still large and heavy, and they are not able to provide

large grasp force, compared to the human hand. Robotic hands can be classified based on several criteria. Considering the type of actuation, most commonly used type of actuators are servos. The vast majority of robotic hands, including the one presented in this paper use this type of actuators [4-9, 11]. Servos are suitable for control but have poor mass/payload ratio. Pneumatic artificial muscles (PAMs) are lightweight and have much better mass/payload ratio than electric motors. PAMs have similar force characteristic as human muscles, but the characteristic is nonlinear. The great advantage of PAMs is their intrinsic compliance, but they need compressed air, which limits the mobility and manipulability of such robotic hands. Several dexterous robotic hands that use PAMs for actuation have been developed [10, 12]. Another solution of the lightweight artificial hand design, with special flexible fluidic actuators, is reported in [13]. An innovative design has been proposed for a robotic hand, which uses so-called hydraulic cluster actuators [14]. This electro-hydrostatic actuator generates great force, more than 260 N. Besides above-mentioned actuators, some other types of actuators might also be used like: piezoelectric actuators, memory alloys, and electro-active polymers.

### *1.2. Contribution of the paper*

The main contribution of this paper is the development and implementation of the BDC motor position controller for actuating robotic hand's joints. First, the fuzzy based position-velocity control algorithm is developed in Matlab/Simulink and the algorithm is later implemented on to the real-time embedded ARM Cortex M4 platform. The performance of the controller in simulation and the real world has been evaluated, and the fuzzy based controller has been compared with respect to the classical PID cascade position velocity controller.

This paper is organized as follows. In section 2, first, the mechanical design of the FTN robotic hand is briefly described. After that, the proposed electronic system for actuation is introduced, with a special emphasis on the implementation issues and prototype design. The used methodology is briefly discussed in section 3, where the model of actuators is introduced and the experimental platform is described. In section 4, the comparison of the proposed fuzzy-based position controller and the traditional PID controller is presented, both in Simulink and on real hardware. At the end of the

paper, in section 5, a brief discussion of the obtained results is given, with a final conclusion.

## 2. Mechanical and electronic control design of the hand

### 2.1. Mechanical design of the hand

FTN robotic hand, with its biologically inspired design and kinematic structure, was originally presented in [15]. It has 5 fingers, where each finger has 3 joints (3 DOFs) which provide the flexion/extension movement.

The thumb has 3 DOFs for flexion/extension and additional DOF for the rotation in its base. Kinematic

parameters of the hand are shown in Fig. 1. a) and CAD model is shown in Fig. 1. b), c).

In order to provide a lightweight structure of the hand, all finger segments and the palm are supposed to be realized on a 3D printer. This production technique is suitable for rapid prototyping and allows complex shapes to be realized in order to provide anthropomorphic appearance and compact design. Unlike most robotic hands which have actuators located in the forearm, the hand proposed in this paper has 5 brushed DC motors embedded in the palm (Fig. 1. c). Since only 5 motors are used for actuation of 16 joints, the hand is highly underactuated.

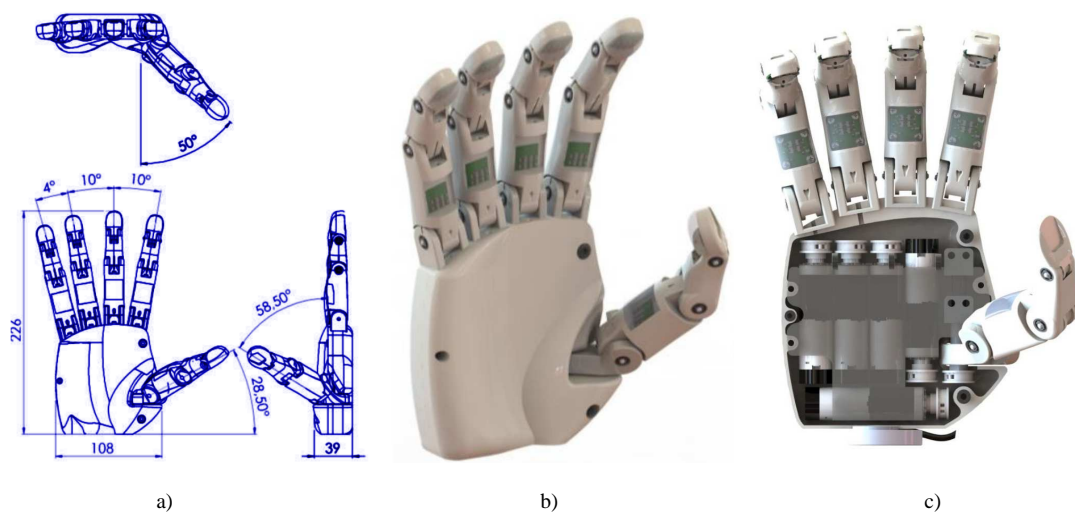


Fig. 1. FTN robotic hand: a) Structure of the hand and its kinematic parameters; b) CAD model of the robotic hand and c) actuation system embedded in the palm

Middle finger and the index finger are actuated with one motor, each, while the thumb has one motor for flexion/extension movement and another one for the rotation in its base. The tendon-driven mechanism is used for the flexion/extension of each finger and these movements are actuated by the motors located in the palm. Each tendon goes from the pulley on the motor shaft in the palm, through the guiding holes in each finger's segments to the fingertip, where it is fastened. Tendons and springs in joints impose constraints on finger motion and provide coupled motion in finger joints. In order to minimize the friction in the finger joints, small radial ball bearings are integrated into each joint. The rotation in the base of the thumb is also tendon driven. Two pulleys were used for power transmission in the base joint of the thumb. Unlike the other joints, tendon mechanism

rotates the thumb joint in both directions, without a spring.

In each finger joint, there is a torsional spring. Hence, the finger flexion is realized by DC motor, as a single active element, while the extension is realized by torsional springs, as antagonistic passive elements. The stiffness coefficients of these springs define the trajectory of the finger and the way it bends during unconstrained motion, in the absence of external forces and obstacles. This tendon-driven mechanism with springs provides certain passive adaptability to the shape of the object that is being gripped. If the first finger segment hits the obstacle, while bending, the second and third segment will continue to bend, until they hit the obstacle or reach their mechanical limits.

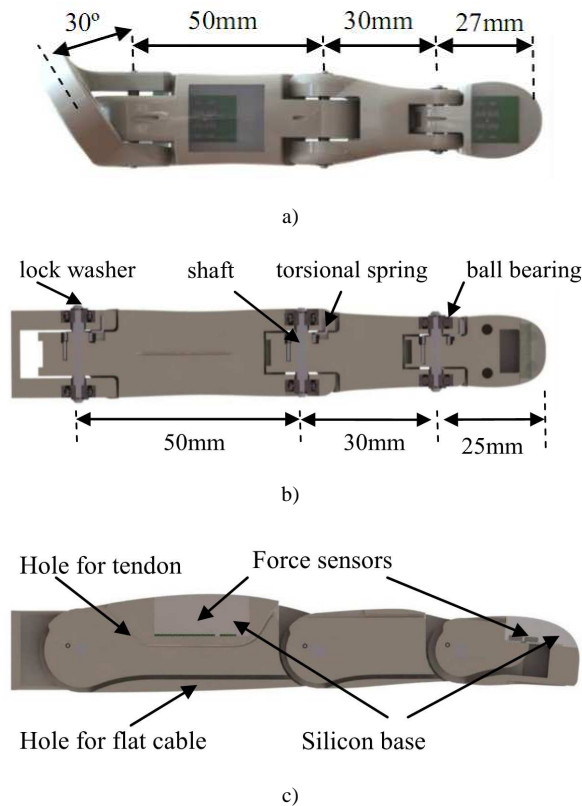


Fig. 2. Kinematic parameters of the fingers a) frontal view of a thumb; b) frontal and c) lateral view of other fingers

Mechanical design of the finger joints is shown in cross section in Fig. 2. There are two radial ball bearings in each joint and a torsional spring. Small lock washers are used to constrain the axial movement of the joint shafts. Flat cables for force sensors [16] and steel tendon for finger actuation are led through finger segments through guiding holes.

## 2.2. Implementation of electronic system for actuation of BDC motors

One of the most important objectives is to design robotic hand that is highly anthropomorphic and biologically inspired by the human hand. This task is challenging from the implementation point of view, considering the necessary electronic system for the actuation of DC motors. In order to provide systematic design, the basic requirements that a system must meet are defined:

- The system must support the actuation of eight BDC motors.
- Fast full-duplex communication is required.

- The Very powerful processor needs to handle a large amount of data in real time.
- The system must have its own power supply for electronic components.
- Debugging support.
- The spatial dimensions of the system must fit into a very small space.

Since the available space for the installation of actuation printed circuit board (PCB) is very small, the last requirement is the most challenging [17-19]. In order to fulfill this requirement, along with other constraints and demands, an extensive analysis of available integrated circuit (IC) solutions has been performed. Besides the necessary functionality, other criteria for the IC selection process were: (i) its physical dimensions and (ii) the number of required external (mostly passive) components. Clearly, the smaller IC that requires less external components represents a better solution. Also, the dimensions of the external components were considered. In Fig. 3, a block diagram with selected ICs and their mutual connection is shown.

For actuation of finger segments, a brushless DC motor from Maxon motor manufacturer is chosen. From the standpoint of electronic system design, the most important characteristics of the chosen BCD motor are the power of 1.2 W, the nominal voltage of 12 V, the maximum continuous current of 210 mA and starting current of 386 mA.

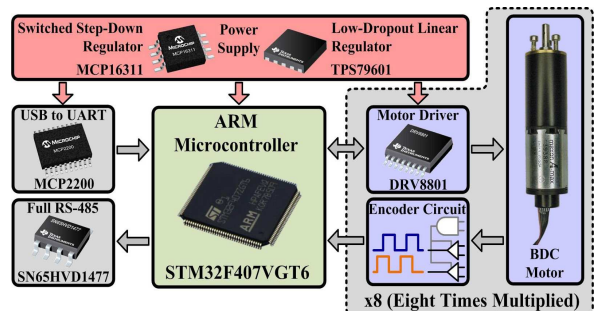


Fig. 3. Block diagram of electronic system for actuation of BDC motors with manufacturer part number of the main components

Specialized integrated component DRV8801 from Texas Instruments manufacturer was chosen as the optimal solution because it requires only a few external components. It is suitable for the selected BDC motor and has a lot of features that are extremely important for the intended application. IC contains a full H-bridge with integrated N-channel MOSFETs, the internal charge pump, 100% PWM support, wide supply voltage range (8 V to 36V) and lot of im-

portant protection features such as: undervoltage lockout (UVLO), charge pump under-voltage (CPUV), over current protection (OCP), short-to-supply and short-to-ground protection, overtemperature warning (OTW), over-temperature shutdown (OTS) and fault condition indication pin (nFAULT). Typical application circuit and connections to the microcontroller are shown in Fig. 4. The microcontroller uses seven pins for full control of the driver circuit. Signal VPROPI represent voltage output proportional to winding current and it must be connected to ADC pin. Another feedback signal is nFAULT which pulls logic low in a fault condition. It is open-drain output so it must be pulled-up to the appropriate voltage. Signals MODE1, MODE2, PHASE, ENABLE and nSLEEP are used to program different functionality of the driver circuit.

The electronic system for hand management is designed to perform most operations locally. However, for the proper operation of the entire robot system, it is necessary that the components mutually exchange information. The amount of information can be very large so it is necessary to provide fast and reliable communication. These are the main reasons for the selection of a full-duplex RS-485 standard for communication. For the implementation of this standard Texas Instrument's SN65HVD1477 IC in a small package for demanding industrial applications has been chosen. The bus pins are robust to ESD events, with high levels of protection to human body model (HBM) and IEC contact discharge specifications.

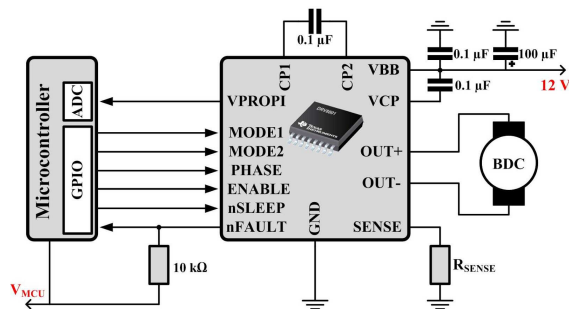


Fig. 4. Schematic with DRV8801 BDC motor driver

For debugging purposes, a USB-to-UART serial converter is introduced. The MCP2200 IC from Microchip manufacturer is a serial converter which enables USB connectivity in the application that has a UART interface. The device reduces external components by integrating the USB termination resistors.

In this way, it is possible to follow in real time the execution of the program in the microcontroller.

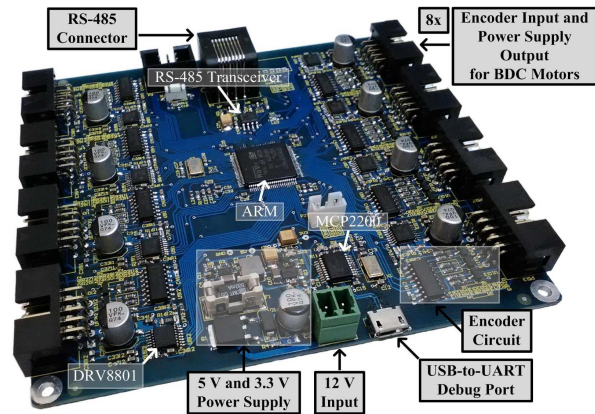


Fig. 5. Prototype board for development of control algorithms for 8 BDC motors

For normal functioning of all parts of the electrical system, it is necessary to provide a stable supply of 3.3V and 5V. In order to avoid unnecessary waste of energy, a switched step-down power supply, that provides 12V to 5V voltage regulation, is designed. The MCP16311 IC from Microchip as a solution with the maximum output current of 1A, up to 95% efficiency, fast transient response, small PCB footprint is chosen. For 5V to 3.3V conversion, a low-dropout linear regulator TPS79601 from Texas Instruments is selected as a component that provides ultralow-noise support, up to 1 A current output, high power supply rejection ratio (PSRR) and very low quiescent current. The dimension of IC are 3 x 3 mm and with only a few external component makes the perfect solution for space required an application. The prototype PCB board is shown in Fig. 5.

### 3. Methodology

The process of development of the proposed controller has two stages. In the first stage, modeling and simulation are used for rapid development of controller. A brushed DC motor is modeled, and a fuzzy controller is designed in Matlab/Simulink environment. In the second stage, the experiment is conducted on a real hardware, with the developed controller implemented in C language for ARM Cortex M4 controller [20]. This way, the controller designed in simulation environment could be verified in the real world and the results between outputs can be compared.

### 3.1. Modeling of the actuators

The custom made Maxon A-max brushed DC motor, used in the project to actuate the fingers of the robotic hand, is modeled in Simulink. The second order model of the brushed DC motor is used. It is described by the following equation:

$$J\ddot{\theta} + b\dot{\theta} = K_m i$$

$$L\frac{di}{dt} + Ri = U - K_e\dot{\theta}$$

where  $J$  is rotor inertia,  $b$  is viscous friction,  $K_m$  is torque constant,  $L$  is terminal inductance,  $R$  is terminal resistance, and  $K_e$  is speed constant. The values of the parameters of the used motor [21] are given in the following table:

Table 1

Values of the parameters for modeling DC motor

Parameter	Value	Unit
Rotor inertia - $J$	0.857	gcm <sup>2</sup>
Viscous Friction - $b$	0	Nms
Torque constant - $K_m$	10.7	mNm/A
Terminal inductance- $L$	1.13	mH
Terminal resistance - $R$	31.1	$\Omega$
Speed Constant - $K_e$	893	rpm/V

Rotary incremental encoders (quadrature) connected to the rotor shaft convert rotational motion to digital information in the form of pulse signals. The encoder [22] is modeled using the following specifications:

- counts per revolution: 512,
- number of channels: 3,
- maximum operating frequency: 320kHz.

### 3.2. Experimental platform

In Fig. 6 the experimental platform used for development and verification of control algorithms is shown. The setup is composed of a control board that is described in detail in section 2.2., and a tendon-driven finger with 3 DOFs actuated by a BDC motor with incremental encoder. The parameters of the motor and encoder are equal to those used in modeling for the purpose of the simulation.

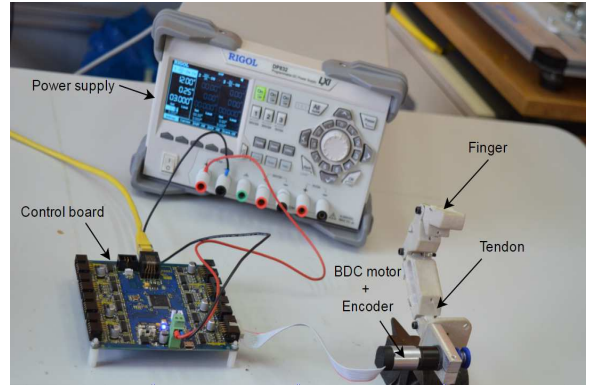


Fig. 6. Experimental prototyping platform

Additionally, the experimental platform has a power supply, and a connection to a PC computer, for programming, debugging and communication with the control board.

## 4. Fuzzy based position velocity controller and comparison with traditional PID controller

### 4.1. PID controller

To compare the results obtained with the fuzzy controller, first, a classical position-velocity controller using PID rules is developed [23, 24]. For tuning the controller, a Ziegler-Nichols method is used. As a first demonstration example, position controller for a DC motor is described below. In this example, a PID controller is used to move a DC motor shaft from its initial position (0) to the final position (90 [rad])<sup>1</sup>. Fig. 7 shows the response of a Simulink model of PID control loop for the position control of a DC motor.

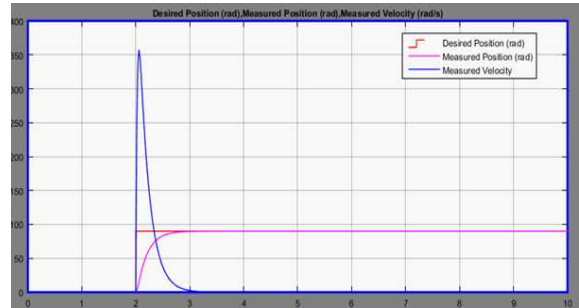


Fig. 7. Response of PID position controller tuned by Ziegler-Nichols method

<sup>1</sup> The position is controlled and measured on a motor side, i.e. before the reduction.

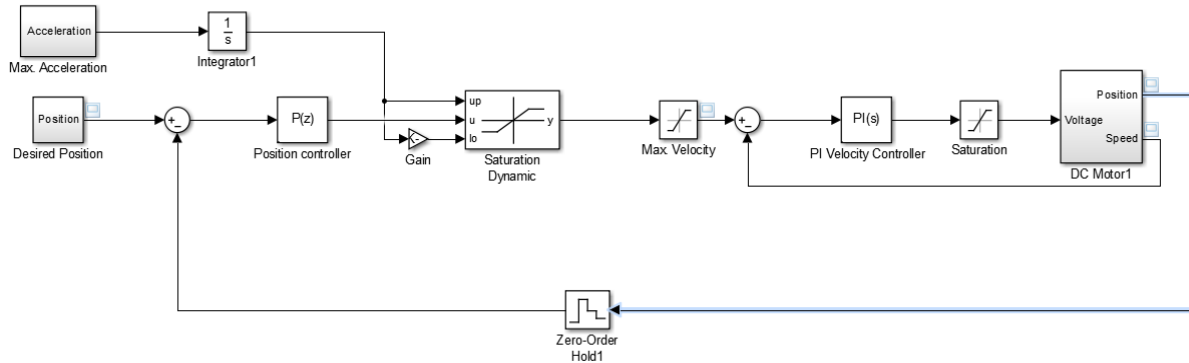


Fig. 8. Simulink model of cascaded position-velocity control

From the response it can be seen that the controller allows the DC motor to achieve its target position, but the velocity increases and decreases rapidly, causing an overshoot in the position before reaching the target position. Such transient behavior could cause problems in the real hardware implementation of the finger actuation system. The actuation has to be slow and controlled, and not fast with a significant jerk.

The problem with the previous position control system is that the velocity immediately spiked up and came down in order to achieve the target position. However, what is actually needed is a slower, and smoother movement from initial position to the desired position. One way to achieve this is to use a position-velocity controller with an embedded velocity profile. Thus, the Simulink model shown in Fig. 8 introduces a cascade position-velocity controller in order to achieve this controlled movement of the motor position.

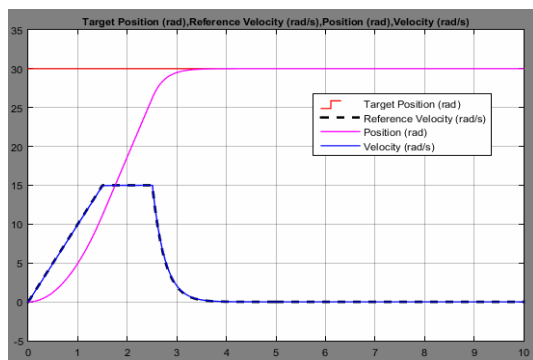


Fig. 9. Output of Position Control using cascaded PI controller

There are two controllers and two control loops in this model. The outer loop has the position controller and inner loop has the velocity controller. Parameters like the initial position, target position, maximum velocity, and acceleration provide a velocity profile for motor movement from initial to the final position. Fig. 9 shows the obtained velocity profile in order to move the motor from its initial position (0 [rad]) to final position (30 [rad]) without a jerk at the beginning and at the end of the motion.

It can be observed from the output that the measured velocity follows the trapezoidal velocity at the beginning of the motion and helps the motor reach its desired position in a controlled manner.

#### 4.2. Fuzzy controller

In this section, a Fuzzy Logic controller [25] is described for controlling the position of a motor [26] and it is compared with the classical PID control technique presented in Section 4.1. For implementing Fuzzy Logic controller, the following Simulink model shown in Fig. 10 was designed, following previous applications and theoretical aspects of fuzzy Control [27, 28].

It can be observed from the figure that for achieving the desired position, a position controller is used in the outer loop and a Fuzzy velocity controller is used in the inner loop. The output from the position controller along with the desired acceleration and maximum velocity generates the velocity profile similar as in the case of a controller shown in Fig. 9. The Fuzzy controller has to control the output speed along this generated velocity profile in order to achieve the desired position.

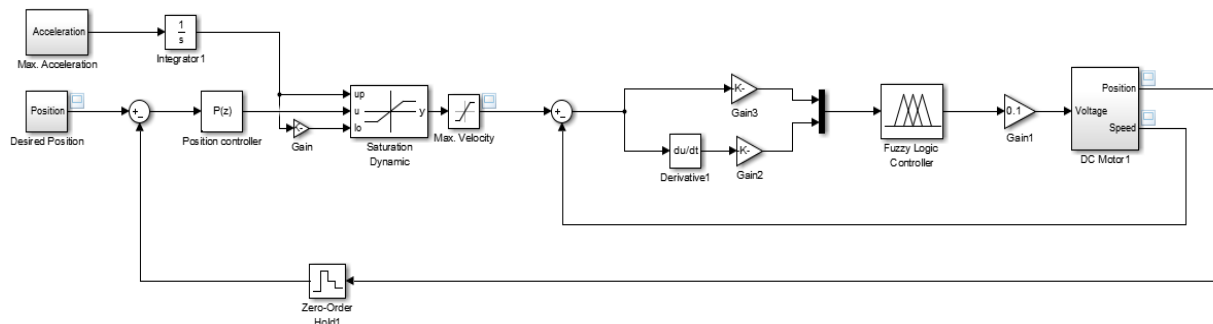
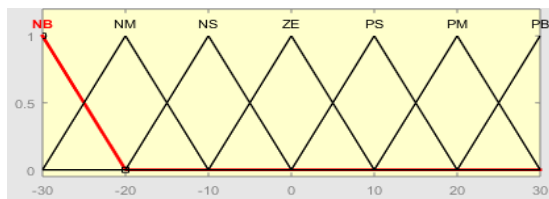


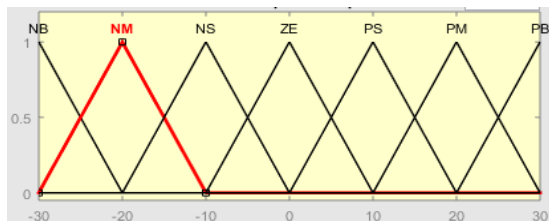
Fig. 10. Position-velocity motor controller using Fuzzy Logic Controller

For the Simulink model of the Fuzzy Logic controller described in Fig. 10, two input parameters are required. The two parameters are “Error” and “Change in Error”. A Mamdani Fuzzy Inference System was used for modeling this controller. The Triangular membership functions are used to define the degree of membership of the input and output variables as described in Fig. 11.

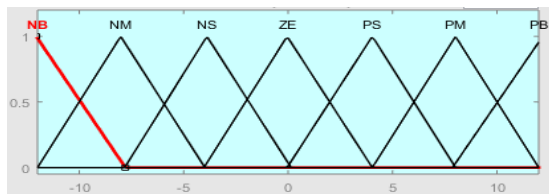
A rule base was formulated in order to define the controller functionality. It is of the “If - Then” format, where the “if” part represents the condition and the “then” part represents the conclusion. The various measured inputs are compared against each other using this rule base and the output is generated according to the rule base described below in Fig. 12.



a)



b)



c)

Fig. 11. Membership Function plot of input variable a) ‘Error’, input variable b) ‘ChangeInError’, and output variable c) ‘output’

E \ CE	NB	NS	ZE	PS	PB
NB	NB	NB	NB	NS	ZE
NS	NB	NB	NS	ZE	PS
ZE	NB	NS	ZE	PS	PB
PS	NS	ZE	PB	PB	PB
PB	ZE	PS	PB	PB	PB

Fig. 12. Rule Base

This is a control system which has 2 inputs E (error) and CE (change in Error) and 5 membership functions NB (Negative Big), NS (Negative Small), ZE (Zero Error), PS (Positive Small) and PB (Positive Big). The rules of this system can be read as: “If E is NB and CE is NB then the output is NB”, “If E is NS and CE is NB then the output is NB” etc. After Fuzzification is completed, we use the rule base to map the input variables to linguistic output variables. But the linguistic output variables cannot be fed into the device and hence has to be converted back into a numeric value and this process is called Defuzzification. The Defuzzification method used here was the center of gravity method.

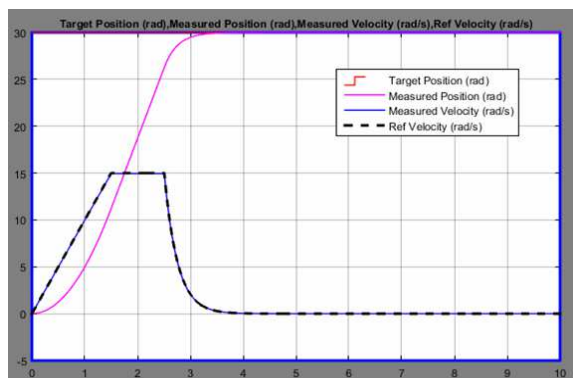


Fig. 12. Output of motor position control using Fuzzy Logic Controller

It can be observed from the output in Fig. 12 that the measured velocity follows the trapezoidal velocity profile at the beginning of the motion and helps the motor reach its desired position in a controlled manner.

#### 4.3. Implementation of real time control system and comparison of the results

For the purpose of experimental verification, both, the PID and a Fuzzy Logic controller are implemented on real hardware. In the chosen case study, the controller was set to move the motor shaft position from 0 to 100 [rad], with a maximum acceleration of 0.75 [rad/s<sup>2</sup>], and a maximum velocity of 6 [rad/s]. Both controllers were first tested in a simulation environment and later on an embedded platform. The obtained results are discussed at the end of this section. The output from the PID controller and Fuzzy controller in simulation environment are shown in Fig. 13 and Fig. 14.

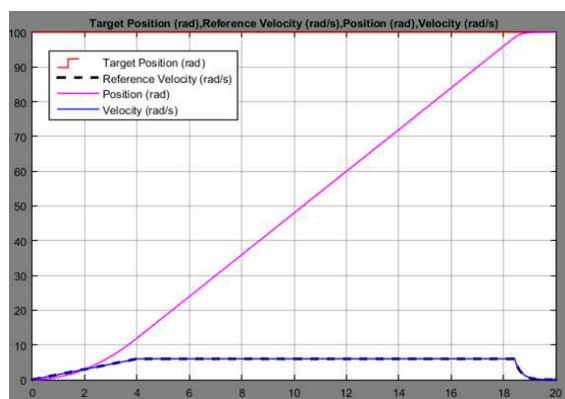


Fig. 13. Output of cascaded PID controller in a simulation environment

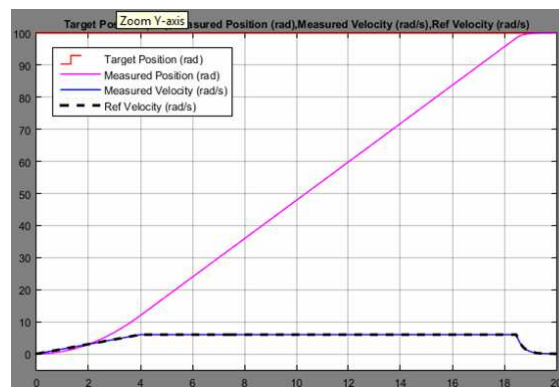


Fig. 14. Output of cascaded Fuzzy Logic Controller in a simulation environment

The result obtained from the cascaded PID controller while testing on hardware is shown in Fig. 14. The resulting graph was generated by plotting the values of the reference velocity, measured velocity and measured position obtained from experimental platform every 1ms. The result obtained from the cascaded Fuzzy Logic controller while testing on the experimental platform is shown in Fig. 15. The resulting graph was also generated by plotting the values of reference velocity, measured velocity and measured position obtained from experimental platform every 1ms.

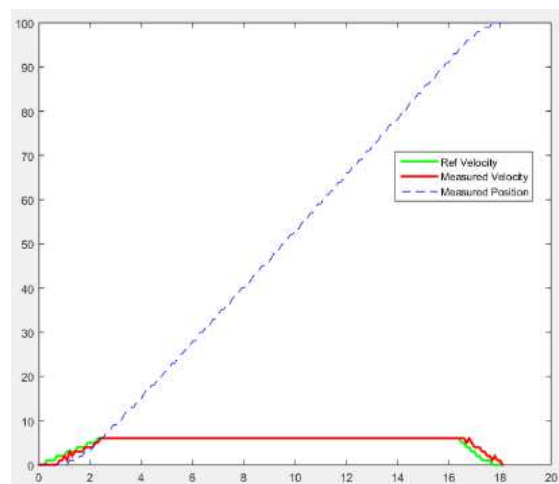


Fig. 14. Output of the implementation of PID controller on an experimental platform

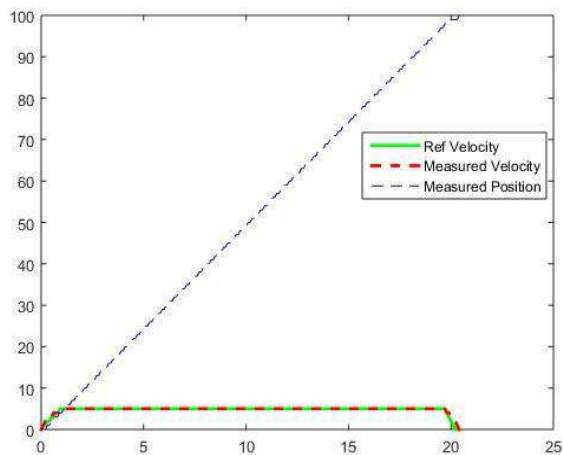


Fig. 15. Output of the implementation of Fuzzy Logic controller on an experimental platform

#### 4.4. Discussions

From the results of both PID controller and Fuzzy Logic controller on the experimental platform, it can be observed that there is not much of a difference in the characteristics of both types of controllers in the time domain, however, it could be observed that the Fuzzy logic controller displayed slightly better rise time and settling time.

The PID controller performed well in controlling the velocity of the motor along the desired velocity profile in order to achieve the target position from its initial position. The performance of the PID controller could be improved a bit more by additional tuning of the parameters manually.

The Fuzzy Logic controller showed good performance in controlling the velocity along a similar velocity profile generated by setting the initial position, desired position, desired velocity and maximum acceleration. The main advantage of a Fuzzy Logic controller is that an exact mathematical model is not required for designing a Fuzzy controller. Also since it is expressed in a linguistic manner [29], it is easily understandable.

Fuzzy Logic Controller has the advantage that it can work well with nonlinear systems [30]. However, compared to PID controller which has only three parameters, the Fuzzy controller has a lot of parameters to be taken into account. The number of membership functions and the rule base plays a vital role in how the controller responds. It was observed that the shape of the membership function selected didn't make much difference, but specifying the

degree of membership of the inputs and the outputs accurately makes a lot of difference.

One problem observed with the Fuzzy controller is that the computational time needed to obtain the new control variable was much greater for the FLC than the PID controller due to the Fuzzification and Defuzzification involved.

#### 5. Conclusion

A DC motor was successfully modeled in Simulink and control algorithms using PID controller and Fuzzy Logic controller were implemented and tested. Both the controllers displayed identical characteristics in the simulation but the FLC took more time to complete execution. Both these controllers were later implemented and tested on an embedded level using the STM32F4 microcontroller. Fuzzy Logic controller and the classical PID controller both displayed similar characteristics in the time domain although the Fuzzy Logic controller displayed slightly better Rise-time and Settling-time.

The Fuzzy Controller could be an alternative to the classical PID controller where the system is nonlinear. A mathematical model of the system is not required to model a Fuzzy Logic controller. Computational time is a problem with the real-time Fuzzy logic controller. More membership functions would mean better control but longer computational time. Hence, the Fuzzy Logic controller can be considered as a replacement for the classical PID controller in all nonlinear systems.

#### Acknowledgment

This work is supported by EU H2020 project 752611 – ACTICIPATE, EU Erasmus+ program between UNS and SRH-Heidelberg and by scientific funds of Republic of Serbia under Grant III44008.

#### References

- [1] J. R. Napier, "The prehensile movements of the human hand," *Journal of Bone and Joint Surgery*, Vol. 38B, Num. 4, pp. 902-913. 1956.
- [2] C. L. Taylor, R. J. Schwarz, "The anatomy and mechanics of the human hand", *Artificial Limbs*, Vol. 2, Num. 2, pp. 22-35, 1955.
- [3] J. W. Soto Martell, G. Gini, "Robotic Hands: Design Review and Proposal of New Design Process," *Proc. of World Academy of Science: Engineering & Technology*, Vol. 20, pp. 85, 2007.

- [4] C. S. Lovchik, M. A. Diftler, "The Robonaut Hand: A Dexterous Robot Hand For Space", Proc. International Conference on Robotics and Automation, Detroit, Michigan, vol. 2, pp. 907-912, 10-15 May 1999.
- [5] L.B. Bridgwater, C. A. Ihrke, M. A. Diftler, M. E. Abdallah, N. A. Radford, J. M. Rogers, S. Yayathi, R. S. Askew, D. M. Linn, "The Robonaut 2 Hand – Designed To Do Work With Tools," Proc. International Conference on Robotics and Automation, Saint Paul, MN, pp. 3425-3430, 14-18, May 2012.
- [6] J. Butterfaß, M. Grebenstein, H. Liu, G. Hirzinger, "DLR-Hand II: Next Generation of a Dexterous Robot Hand," Proc. International Conference on Robotics and Automation, Seoul, Korea, pp. 109-114, 21-26, May 2001.
- [7] H. Liu, K. Wu, P. Meusel, N. Seitz, G. Hirzinger M.H. Jin, Y.W. Liu, S.W.Fan, T. Lan, Z.P.Chen, "Multisensory Five-Finger Dexterous Hand: The DLR/HIT Hand II," Proc. IEEE/RSJ International Conference on Intelligent Robots and Systems, Nice, France, pp. 36923697, 22-26 Sept. 2008.
- [8] T. Mouri, H. Kawasaki, K. Yoshikawa, J. Takai, and S. Ito, "Anthropomorphic Robot Hand: Gifu Hand III," Proc. International Conference on Control, Automation and Systems, Muju Resort, Jeonbuk, Korea, pp. 1288-1293, October 16-19, 2002.
- [9] F.Lotti, P.Tiezzi, G.Vassura, L.Biagiotti, C.Melchiorri, "UBH 3: an anthropomorphic hand with simplified endo-skeletal structure and soft continuous fingerpads," Proc. International Conference on Robotics and Automation, Barcelona, Spain, vol. 5, pp. 4736-4741, 26 April-1 May 2004.
- [10] <https://www.shadowrobot.com/products/dexterous-hand/>, last time visited on Jun 6th 2017.
- [11] <http://elumotion.com/index.php/portfolio/project-title-1>, last time visited on Jun 6th 2017.
- [12] G. Gini, M. Folgheraiter, I. Baroni, F. Boschetti, G. Petja, M. Traversoni, "A biomimetic upper body for humanoids," Proc. Robotics (ISR), 2010 41st International Symposium on and 2010 6th German Conference on Robotics (ROBOTIK), Munich, Germany, pp. 1-8, 7-9 June 2010.
- [13] S. Schulz, C. Pylatiuk and G. Bretthauer, "A New Ultralight Anthropomorphic Hand," Proc. IEEE International Conference on Robotics and Automation, Seoul, Korea, pp. 2437-2441, 21-26 May 2001.
- [14] T. Kang, H. Kaminaga, Y. Nakamura, "A robot hand driven by hydraulic cluster actuators," Proc. IEEE-RAS International Conference on Humanoid Robots, Madrid, Spain, pp. 39-44, 18-20 Nov. 2014.
- [15] Savić, S., Raković, M., Penčić, M., Nikolić, M., Dudić, S., Borovac, B. Design of an Underactuated Adaptive Robotic Hand with Force Sensing. International Conference on Electrical, Electronic and Computing Engineering IcETRAN, Zlatibor; 2016
- [16] M. Raković, M. Beronja, A. Batinica, M. Nikolić, B. Borovac, "3 axis Contact Force Fingertip Sensor based on a Hall effect Sensor," Proc. IFToMM/IEEE/euRobotics 25th International Conference on Robotics in Alpe-Adria-Danube Region – RAAD 2016, Belgrade, Serbia, 30 June – 2 July 2016.
- [17] S. J. Haddadi and P. Zarafshan, "Design and fabrication of an autonomous Octorotor flying robot," 2015 3rd RSI Int. Conf. on Robotics and Mechatronics (ICROM), Tehran, 2015, pp. 702-707. doi 10.1109/ICRoM.2015.7367868
- [18] Kecskés, I., Burkus, E., Bazsó, F., & Odry, P. (2017). Model validation of a hexapod walker robot. *Robotica*, 35(2), 419-462. doi:10.1017/S0263574715000673
- [19] Bellicoso, C. D., Buonocore, L. R., Lippiello, V., Siciliano, B. "Design, modeling and control of a 5-DoF light-weight robot arm for aerial manipulation". In *Control and Automation (MED)*, 2015 23th Mediterranean Conference on (pp. 853-858). IEEE., June, 2015,
- [20] Joseph Yiu , *Definitive guide to ARM cortex M3 and ARM cortex M4 Processors*, Newnes Publishers, 2013
- [21] Maxon DC Motor / May 2012 edition - A-max 16 Ø16 mm, Precious Metal Brushes CLL, 1.2 Watt (Article number: 110056)
- [22] Maxon sensor / May 2012 edition - Encoder MR Type M, 128–512 CPT, 2/3 Channels, with Line Driver (Article number: 201940)
- [23] Zhong, J. (2006). PID controller tuning: a short tutorial. class lesson), Purdue University.
- [24] Araki, M. (2010). *Control Systems, Robotics and Automation—vol II—PID Control*. Kyoto University, Japan.
- [25] Kecman, V. (2001). *Learning and soft computing: support vector machines, neural networks, and fuzzy logic models*. MIT press
- [26] E. Mamdani, "Advances in the linguistic synthesis of fuzzy controllers", *Int. Journal of Man-Machine Studies*, 8(6):669–678, 1976.
- [27] Y. Li, C. Lau, "Development of fuzzy algorithms for servo systems", *IEEE Control Systems Magazine*, Vol. 9., No. 2, pp. 65–72, April 1989.
- [28] R. J. Marks, editor. *Fuzzy Logic Technology and Applications*. IEEE Press, New York, 1994.
- [29] H. T Nguyen, M. Sugeno, R. Tong, R. R. Yager, editors, *Theoretical Aspects of Fuzzy Control*, Wiley, New York, 1995.
- [30] I. W. Sandberg, K. K. Johnson, "Steady state errors in nonlinear control systems", *IEEE Trans. on Automatic Control*, Vol. 37, No. 12, pp. 1985–1989, December 1992.